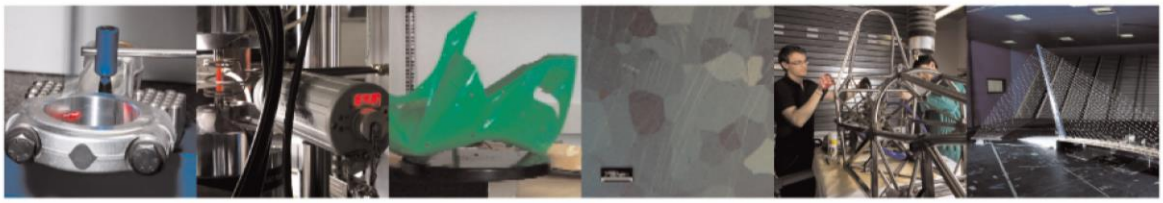

Extrusion of metal powder-polymer mixtures: Melt rheology and process stability

Strano, M.; Rane, K.; Briatico Vangosa, F.; Di Landro, L.

This is a post-peer-review, pre-copyedit version of an article published in JOURNAL OF MATERIALS PROCESSING TECHNOLOGY. The final authenticated version is available online at: http://dx.doi.org/10.1016/j.jmatprotec.2019.116250

DIPARTIMENTO DI MECCANICA ■ POLITECNICO DI MILANO
via G. La Masa, 1 ■ 20156 Milano ■ EMAIL (PEC): pecmecc@cert.polimi.it
http://www.mecc.polimi.it
Rev. 0

Extrusion of metal powder-polymer mixtures: melt rheology and process stability

Matteo Strano[a*], Kedarnath Rane[a], Francesco Briatico-Vangosa[b], Luca Di Landro[c]

[a]*Dipartimento di Meccanica, Politecnico di Milano, Via La Masa 1, Milano, Italy, kedarnath.rane@polimi.it*

[b]*Dipartimento di Chimica, Materiali e Ingegneria Chimica, Politecnico di Milano, Piazza L. Da Vinci, 32, Milano Italy, francesco.briatico@polimi.it*

[c]*Dipartimento di Scienze e Tecnologie Aerospaziali, Politecnico di Milano, Via La Masa 34, Milano, Italy, luca.dilandro@polimi.it*

**Corresponding author. Tel: +39-0223998520, E-mail: matteo.strano@polimi.it*

Abstract:

The mixture of metal powder and a viscous polymeric binder (often referred to as feedstock) is commonly used for Metal Injection Moulding (MIM) applications. Recently, the interest towards the extrudability of metal/binder feedstocks is increasing, especially because of the growth of additive manufacturing techniques based on the vertical extrusion and layered deposition of filaments. In this experimental work, a feedstock prepared as a mixture of stainless steel 316L powder with water-soluble binder was tested. The rheological behaviour of different mixtures (with powder loading between 50 and 63 % in volume) was assessed using a capillary rheometer. The theoretical window of optimal extrudability was determined, in terms of temperature, shear rate and powder loading. Then, a specially designed CNC controlled extrusion system was used for performing vertical extrusion tests. The analysis of extrusion pressure profiles and the dimensional variability of the filaments was used to correlate the theoretical extrudability predicted by the rheological model with the actual extrusion tests. All results indicate that the conditions which yield better stability of the extrusion process are those that allow higher viscosity of the mixtures.

Keywords: extrusion; feedstock; shear viscosity; stability; additive manufacturing

1. Introduction

Metal injection moulding (MIM) is an established and recognised manufacturing process, well described and modelled by Gelin et al. (1999), who were among the first investigators of this technology. MIM is used to efficiently produce small near net shape parts with a wide variety of materials. As an example, Raza et al. (2012) produced dog bone shaped stainless steel MIM parts and tested their mechanical properties and corrosion resistance; Sidambe et al. (2102) demonstrated the use of the process for producing commercially pure titanium medical parts, investigating their shrinkage after sintering; Cheng et al. (2010) succesfully fabricated some spherical samples by MIM, using a copper-

tungsten alloy, which resulted with a fine and homogeneous microstructure. Kuang et al. (2009) have shown that the process can even be used for metal matrix composites; they produced some MIM SiC-Ti layered material samples, with a disk shape.

1.1 Processes based on the extrusion of metal/binder feedstock

The raw material for the MIM process is usually called feedstock: it is a mixture of metal powder and a viscous polymeric binder. This kind of feedstock is also used as the raw material for other manufacturing processes. The extrusion of metal-binder feedstock is a less established process, generally used for producing hollow profiles or tubes. Sotomayor and Levenfeld (2010) recently studied the extrusion of thin stainless steel tubes for application in solid oxide fuel cells. Recent developments allow the extrusion based additive manufacturing (EAM), sometimes called freeform deposition, of the feedstock for rapid and dieless production of parts with low production volumes. An innovative machine with a fixed extrusion unit and a robotic deposition table was described in (Annoni et al., 2016), who demonstrated its use for the deposition of steel and ceramic (zirconia) parts. Bose et al. (2018) used the very recent commercial Desktop Metal 3D printer to produce fine, thermally-stable microstructure tungsten alloy part with the potential for very high temperature exercise and high strength, as compared to conventional Tungsten Heavy Alloys. The EAM process for metals enables the production of complex shaped products by growing, layer-by-layer, a green part, to be debinded and sintered afterwards. With this respect, the EAM process of powder/binder feedstock is a hybrid of the conventional Fused Deposition Modeling (FDM) and MIM processes. Parenti et al. (2017) demonstrated that, if required, the 3d printed green parts can be finished by machining in the green state, to achieve better tolerances, prior to debinding and sintering.

1.2 Feedstock composition and preparation

In the three mentioned processes (MIM, extrusion, EAM), the metal powder is first mixed to the so-called binder system. Berginc et al. (2009) presented and compared two different techniques for measuring the rheological properties of MIM feedstocks and showed that the binder concentration varies from 7 to 15 wt.%, depending on the metal powder properties and the geometrical characteristics of the extrusion or moulding dies. The conditions at which the feedstock is prepared and extruded play an essential role in the subsequent part and process characteristics since the binder homogeneity and segregation of powders within the feedstock depends upon these conditions.

The use of water soluble binder systems is particularly interesting, because of the relative simplicity of the debinding operations. Thavanayagam et al. (2015) clarify that the typical water soluble binder has a shear thinning flow

behaviour and it is made of at least three components: a backbone polymer with high melting point (e.g. polyethylene), a soluble wax constituent and a lubricant surfactant (e.g. stearic acid). Polyethylene glycol (PEG) is a frequent selection as the water soluble fraction. Hidalgo et al. (2014) demonstrated that a solid loading up to 65 vol.% is the most equilibrated choice to successfully fabricate Invar 36 MIM parts with a water-soluble binder system based on cellulose acetate butyrate (CAB) and PEG. The use of solvent soluble waxes can be an alternative to PEG: Zaky at al. (2009) demonstrated that a binder system consisting in 35 wt.% polyethylene-co-vinyl acetate (EVA), 62 wt.% of paraffin wax and 3 wt.% of stearic acid is a suitable option for powder compression or injection moulding.

1.3 Flow characteristics of feedstock

The flow characteristics feedstock have been previously studied by some authors for consideration in the injection moulding, extrusion or EAM processes. Huang et al. (2003) investigated the effect of shear rate ($\dot{\gamma}$), solid fraction (either volumetric ϕ_v or by weight ϕ) and temperature (T) on the viscosity. Gonzalez-Gutierrez et al. (2016) proposed some empirical models that can be used to predict the viscosity of polymeric blends as a function of their formulation. While it is universally agreed that the viscosity of feedstock materials is directly related to their processability, very few papers in the scientific literature directly and experimentally investigate the correlations between rheological properties and the processability. As one of the very few available studies, Khakbiz et al. (2005) performed an experimental study via capillary rheometer to estimate the influence of solid loading, shear rate and temperature on the stability of feedstocks for injection moulding, quantitatively evaluated using an "instability index", but did not report any injection moulding test. In (Suri et al., 2003), the flow stability was assessed as the variation over time of the viscosity measured by a torque rheometer. The authors observed that the flow stability is positively influenced by more homogeneously mixed feedstock. Again, the stability was observed only by looking at the results of a rheometer, but no real process observations were correlated. In extrusion, the stability of the process can be regarded either in terms of stability of the pressure vs. time curve (or the stability of viscosity) or in terms of dimensional stability of the extruded filament diameter, which may change due to die swelling and to gravity. Pettas et al. (2015) demonstrated that the dimensional instability of polymer extrusion increases with increasing shear rate and increasing relaxation time. Zauner et al. (2004) have shown that the dimensional stability of powder injection moulded parts can be correlated to the variability of viscosity.

Many papers are also available on the rheology of mixtures made of polymeric binder and ceramic powders. As an example, Faes et al. (2015) investigated the homogeneity, rheology and printability of dispersions containing

22,5%vol to 55%vol ZrO2 mixed with resins. Ismael et al. (2011) investigated the effects of different commercially available thermoplastic binders on the extrudability of highly loaded lead zirconate titanate (PZT) feedstocks. They found that polyethylene-based binders were the most suitable choice. Other relevant papers on ceramics could be cited, but none of these papers has payed particular attention to the flow stability regimes and the limiting extrusion parameters.

1.4 Objectives and organization of the paper

To the authors' knowledge, no literature is available that directly and experimentally relates the rheological properties of metal-polymer feedstock mixtures to their extrudability. The present paper aims at filling this gap. The rheological properties of stainless steel (SS316L) based feedstocks are first determined via capillary rheometer. Then a rheological model is determined and used in order to predict the stability of the mixtures during extrusion. Finally, actual vertical extrusion tests are performed in order to identify the regions of stability of the process.

2. Materials, equipment and methods

2.1 Materials

Stainless steel (SS316L) powder (by Sandvik Osprey) having median particle size D_{50} = 8.8 μm was used as a solid loading in the mixtures, with various volume percentages ϕ_v. The chemical composition of the powder is given in Table 1 and a micrograph of a powder sample is shown in Figure 1a.

A commercial water-soluble binder system (Embemould K83) was used to bind SS316L powder in the feedstock and allow flowability during extrusion and deposition.

The feedstock has been mixed and pelletized, a micrograph of a sectioned pellet is shown in Figure 1b. Contreras et al. (2010) performed a wide experimental campaign to find the optimal solid loading with different powder materials and their work can be used as a reference for evaluating the typical range of solid loading in MIM feedstock as ϕ_v = 50 - 65 %. To accommodate the aforementioned range of ϕ_v, three different mixtures were prepared by mixing SS316L powder and K83 binder to get different volume ratios of SS316L (ϕ_v = 0.49, 0.56 and 0.63, corresponding to weight ratios ϕ = 0.875, 0.900 and 0.925 respectively). According to the study of Kong et al. (2012), this range can be exceeded, i.e. the maximum volumetric solid loading can be increased only in case a smaller particle size is used, e.g. ϕ_v can go up to 70% if D_{50} is below 4 μm.

Table 1: Chemical composition of powder used in the present study

Element	Cr	Ni	Mo	Mn	Si	C	P	S	Fe
Wt.%	17.90	11.70	2.30	1.41	0.72	0.02	0.02	0.006	balance

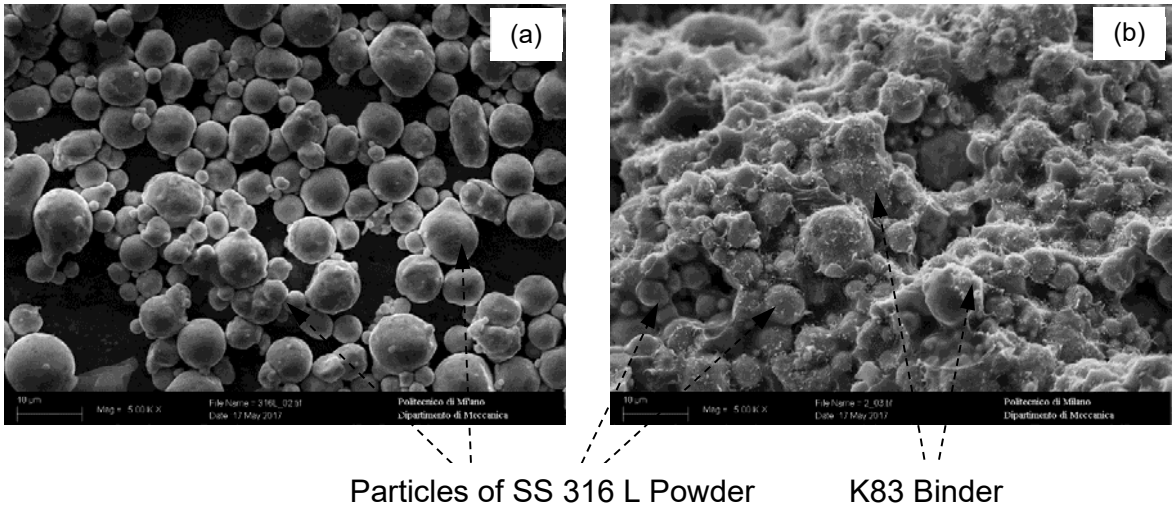

Figure 1: SEM image of (a) SS316L powder and (b) fractured surface of feedstock pellet having 90 wt. % (ϕ_v=56%) solid loading of SS316L powder

The binder system is composed of wax as the major component (melting point ~ 65^{o}C), stearic acid as surfactant and a backbone polymer (polyethylene glycol). Figure 2 shows the DSC diagram of the binder and feedstock mixtures. Pure binder shows distinct peaks corresponding to individual binder constituents. In the feedstock mixture, the binder peaks are significantly lower and shifted leftward, in agreement with previous results in the literature (Samanta et al., 2011). This is due to the presence of SS powder, which interferes with polymer components crystallization during blending.

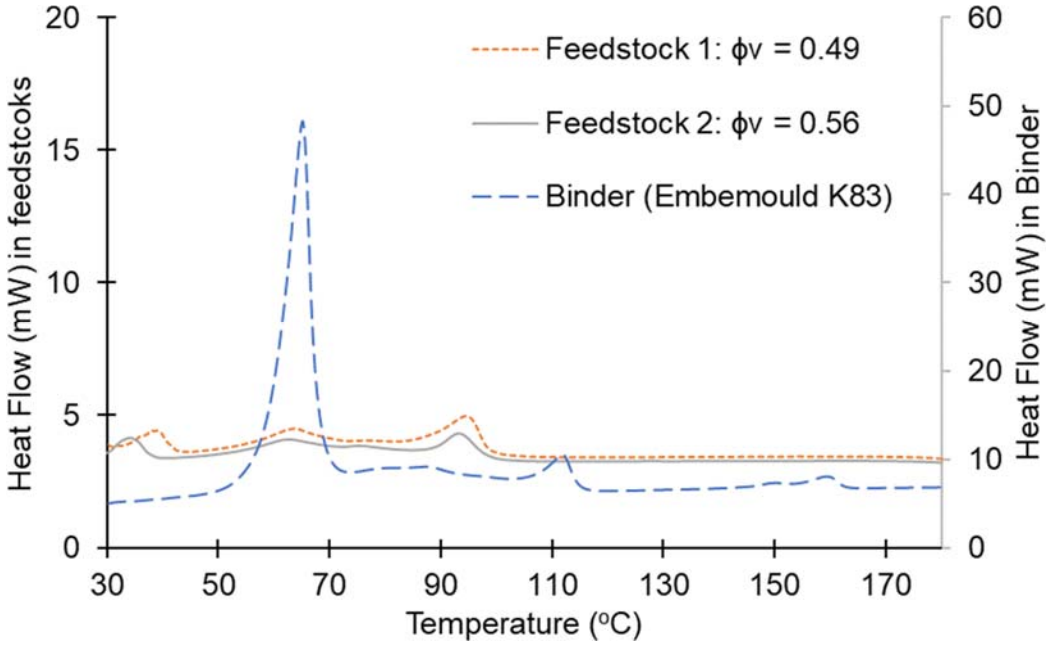

Figure 2: DSC (Endo) thermographs of binder and feedstock used in the present study; to improve the readability of the diagram, the heat flow values for the feedstock mixtures can be read on the left Y-axis, while the larger values obtained for the pure binder can be read on the right Y-axis.

2.2 Rheological equipment

A Rosand capillary rheometer RH 10 (by Malvern Instruments) was used to perform rheological tests for feedstock mixtures. The unit, shown in Figure 3 (a), is comprised of two 15 mm inner diameter barrels equipped with three zones of temperature control. Two parallel pistons extrude the feedstock material placed in the barrels through different capillaries, long capillary (1 mm orifice diameter with 17 mm length) and short capillary (1 mm orifice diameter with 0 mm nominal length). Two pressure transducers were used to measure the pressure at the entrance to the capillary die. Pressure differences measured from these two transducers are used to compensate for capillary entrance/exit losses. The geometrical characteristics of the dies including entrance angle, reduction ratio, and length-to-diameter (L/D) ratio were unchanged for this study.

Various piston speeds were set to obtain the plots of pressure drop vs. flow rate. Flow curves (the extrusion viscosity vs. the apparent shear rate $\dot{\gamma}$) of the various feedstock as a function of extrusion temperature T were obtained from pressure drop vs. flow rate data.

Each feedstock composition has been tested as-mixed (i.e. immediately after its preparation). Then, the same feedstock has been tested again, after being extruded through the capillary nozzle, to verify its rheological modifications after being subjected to the thermo-mechanical history during test.

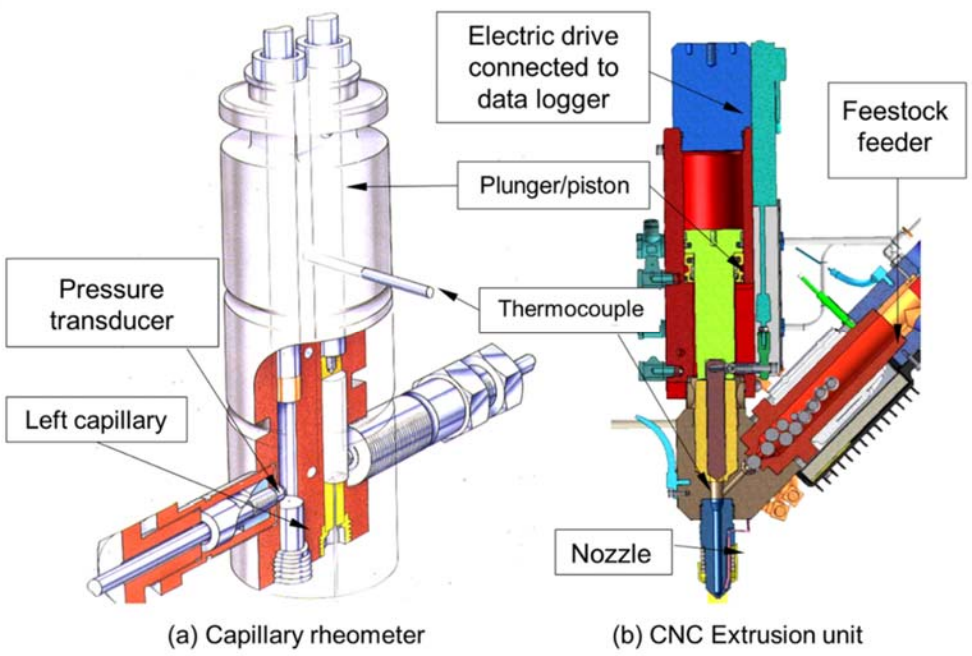

Figure 3: (a) Schematic of capillary rheometer used for the viscosity assessment tests; (b) Computer Numerically Controlled (CNC) extrusion unit for extrusion and EAM tests

2.3 Extrusion tests setup

After rheological testing, an industrial extrusion unit, shown in Figure 3 (b), was used to extrude feedstock filaments of various diameters. The unit, already described in (Giberti et al., 2016) consists of two distinct barrels, respectively for feeding (oriented at 45° to the vertical) and for extruding (vertical). The vertical orientation of the extrusion barrel allows to perform vertical extrusion and deposition on table tests. The feeding cylinder is heated and internally equipped with packed steel balls. The preheated flow enters the extrusion cylinder through a restricted gate. Inside the feeding cylinder, the presence of steel balls and the gate restriction provide shearing and further homogenization of the viscous feedstock. Temperature was measured with thermocouples and controlled at predetermined levels at three different locations: at the feeder barrel, at the extrusion barrel and at the nozzle. The unit is equipped with an extrusion piston, which pushes the material own the barrel and to the extrusion nozzle. The extrusion piston is numerically controlled (CNC), so that its position is known at time intervals of 4 microseconds, with a precision < 0.01 mm. Since

the extrusion piston is controlled in position, the flow rate and shear rate of the extruded material are precisely known, but the pressure variations at the nozzle are not controlled. For this reason, electric current absorption data of the drive unit were stored during extrusion tests and converted into pressure vs. time curves.

Two extrusion nozzles (shown in Figure 4) were used in this study to understand the effect of nozzle geometry on extrusion. The two main nozzle parameters are the throat length L and the throat diameter D_n. Thin D_n conduits and long nozzle increase frictional losses at a lower temperature, due to the high viscosity of the tested feedstock. Conversely, too short throats might favor mid-air bending of the extruded wire (Özgün et al., 2012).

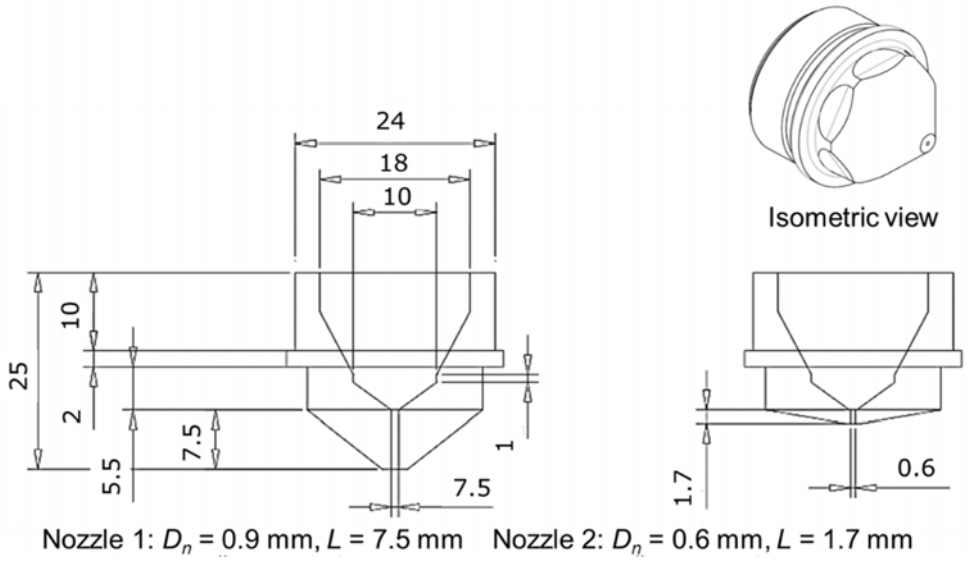

Figure 4: Dimensioned drawings of extrusion nozzles used for present study

Two nozzle diameters D_n (0.9 and 0.6 mm) have been used, to change the flow characteristics, as apparent shear rate $\dot{\gamma}$ decreases with increase in D_n, according to the well known equation (1):

$$\dot{\gamma} = \frac{32Q}{\pi {D_n}^3} \quad (1)$$

where Q is the extrusion volumetric flow rate. Ochoa and Hatzikiriakos (2005), among many other authors, reported that the pressure drop increases with increase in length L, as for equation (2):

$$\tau_w = \frac{\delta P \, D_n}{4 \, L} \quad (2)$$

where τ_w is the wall shear stress and δP is the pressure drop in the capillary length. Nozzle 1 has been selected with larger diameter and smaller D_n/L ratio, to reduce shear rate and increase shear stress with respect to nozzle 2.

After each test, each filament is 180 mm long; both of its ends are trimmed off for a length of 15 mm, and the central 150 mm portion was retained for measurement of filament diameter. Diameters of extruded filaments were measured using a 3D vision measuring machine (by Mitutoyo). All filaments were measured at 8 different locations chosen periodically on the selected length of 150 mm. The mean diameter (D) and its standard deviation (σ_D) were determined from the 8 measurements on each filament.

2.4 Testing parameters

The temperature of the feedstock T at the nozzle has been varied as an experimental parameter both in rheological tests and extrusion tests. Too low an extrusion temperature (below 110ºC) is not feasible because it would require a very high pressure, with a risk of exceeding the available power of the extrusion unit and excessively increase the shear stress. At higher T (above 140 ºC), the binder may degrade inside the feeding and extrusion cylinders and cause a discontinuity in the feedstock flow. A suitable range for T was therefore selected as 110ºC to 140ºC. The complete experimental range and levels for all parameters is reported in Table 2, for both rheological and extrusion tests.

$$\dot{\gamma} = \frac{8\,v_e}{D_n} \tag{3}$$

The resulting equation (3) is obtained by substituting volumetric flow rate, $Q = \frac{\pi {D_n}^2 v_n}{4}$ in equation (1). The range of shear rate for nozzle of diameter 0.9 mm is 177.77 to 720 s^{-1} and for nozzle of diameter 0.6 is 600 to 2413 s^{-1}.

Table 2: Parameter levels used in present experimental study

Solid Loading, ϕ_v	Extrusion Temperature, T (ºC)	Capillary Rheometer	Extrusion Tests	
		Shear rate $\dot{\gamma}$ (s^{-1})	exit velocity v_e (mm/s) at nozzle	
			D_n=0.9 mm	D_n=0.6 mm
0.49 - 0.56 - 0.63	110 - 120 - 130 - 140	10 levels from 50 to 2000	5 levels from 20 to 81	5 levels from 45 to 181

3. Results of Rheological Tests

3.1 Apparent viscosity vs. shear rate, temperature and solid loading

Figure 5 shows the obtained viscosity of feedstocks as a function of shear rate at various temperatures in a log–log scale. All mixtures exhibit a pseudo-plastic or shear thinning behavior, as common for MIM feedstock. The trends are almost linear, which is an indication of stability. The solid loading has a great influence on the rheological behavior

of feedstock. The feedstocks made with a higher concentration of steel powder (ϕ_v = 0.56 and 0.63 volumetric powder content) unsurprisingly have higher viscosity.

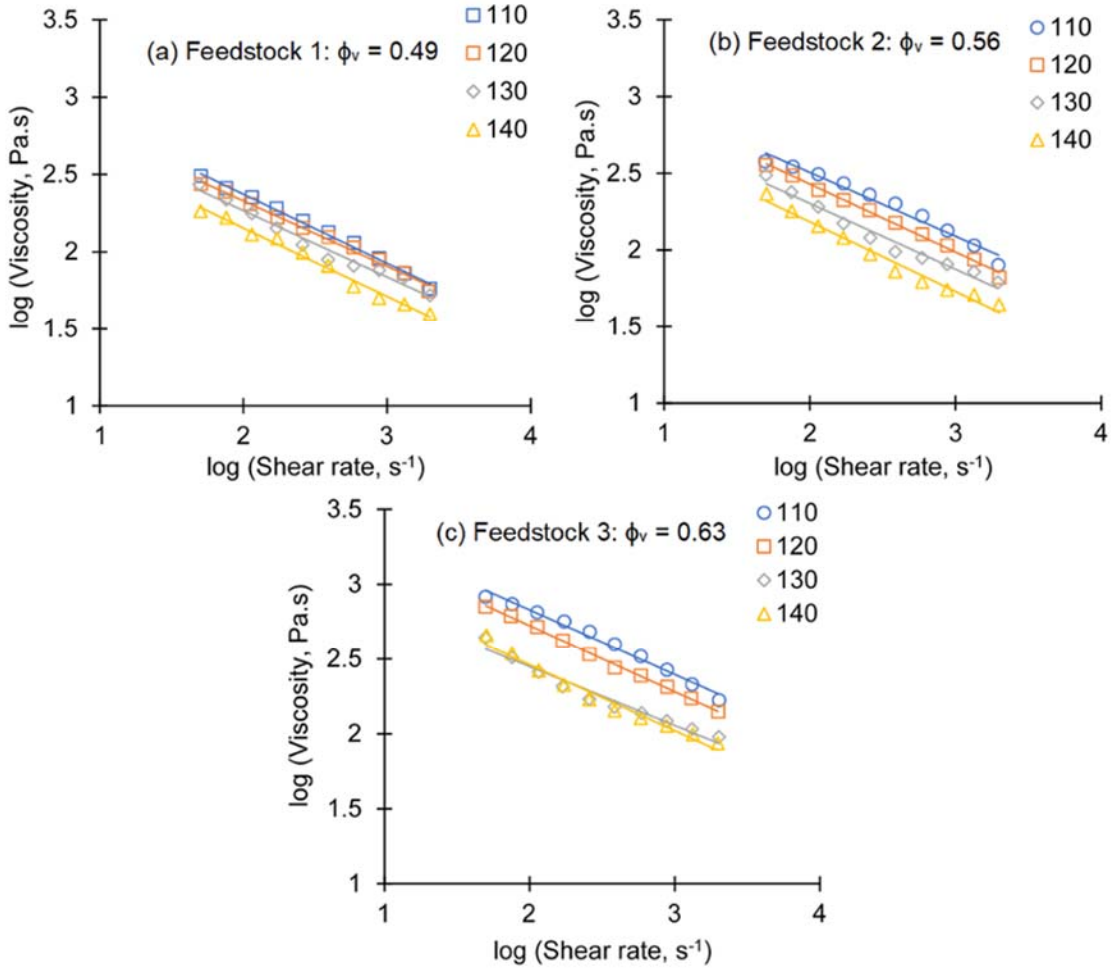

Figure 5: Viscosity of feedstock as a function of shear rate $\dot{\gamma}$ and T (°C) on a log-log scale

A rheological model has been developed by linear regression, that combines into a unique factorial formulation all the relevant effects (solid fraction, temperature *T* and shear rate $\dot{\gamma}$):

$$\eta = \mathrm{K}\left(1 - \frac{\varphi_{\mathrm{v}}}{\varphi_{\mathrm{v\_max}}}\right)^{-\mathrm{m}} \dot{\gamma}^{\mathrm{n}-1} \mathrm{e}^{\mathrm{E/RT}} \qquad (4)$$

The 4 parameters in equation (4) are: the consistency *K* (a constant measured in Pa·s); n and m, which are non-dimensional exponents that model respectively the sensitivity to the shear rate and the solid loading; *E*, which is the flow activation energy (J/mole). *R* is the universal gas constant, the temperature *T* is measured in °K; ϕ_{v_max} is the maximum theoretical relative volumetric density of the given powder under full packing conditions, here assumed as

0.74. The regression model has been developed on the logarithmic terms for the as-mixed feedstocks, yielding the rheological constants listed in Table 3. The model has been re-estimated also on the feedstocks already extruded once. Both models are robust, with normal residual errors and a standard error equal to 1.5 Pa·s a.

Table 3: Coefficients of the 4-parameter rheological model for the as-mixed and the as-extruded mixtures

Constants	As-mixed	As-extruded	Variation after 1st extrusion
K (Pa·s)	0.015	0.025	+63%
m	1.43	0.97	-32%
n	0.55	0.57	+3%
E (J/mol)	32210	32490	+1%

According to equation (4), viscosity is as a non-linearly increasing function of the powder loading ϕ_v. Smaller m-values should be preferable because they reduce the dependence of viscosity on minor variations of feedstock due to inhomogeneity. In powder injection moulding, lower K-values are also preferred because lower consistency facilitates the filling of complex die cavities, as shown by the mouldability indexes proposed in the literature (Machaka et al., 2018). However, in extrusion and deposition processes, the role of the consistency K is not very significant, because there is no cavity to be filled outside the extrusion nozzle. Indeed, larger K-values (i.e. more consistent extruded filaments) are preferable to some extent because it is preferable to have a stable and rigid material, rather than a low viscosity one.

It appears that the extrudability of the analysed powder-binder mixtures improves after the first extrusion, thanks to an increased consistency K and a reduced dependency m on the solid loading, according to Table 3. This improvement, however, cannot be predicted for subsequent extrusions, i.e. the feedstock cannot be recycled indefinitely. In fact, Royer et al. (2015) proved that a degradation of the water-soluble binder can be expected for prolonged exposures at high temperatures.

3.2 Extrudability as a function of solid loading

While the model in equation (4) is compact and robust, it does not allow to investigate what operating conditions (e.g. what level of solid loading) yield the best stability of the extrusion process, i.e. the best extrudability. In fact, a plot of the standardised residuals of the regression model vs. the factors shows a lack of fit of the model with respect to the solid loading ϕ_v. For this reason, a less compact but more accurate representation can be obtained by splitting equation

(4) into three separate 3-parameters models, calculated over the same experimental database, one for each ϕ_v value. A similar approach has been followed by Agote et al. (2001), who evaluated the flowability of different feedstocks using rheological parameters like critical powder volume concentration, viscosity, activation energy, yield stress, power law index and rheological index, with separated models for dependence of the apparent viscosity on the solid fraction from the dependence on temperature T and shear rate $\dot{\gamma}$.

The 3-parameter model can be obtained by fixing the level of ϕ_v as an independent variable and modelling the dependence of the apparent viscosity on the remaining two variables:

$$\eta = \mathrm{K}(\varphi_\mathrm{v})\,\dot{\gamma}^{\mathrm{n}(\varphi_\mathrm{v})-1}\mathrm{e}^{\mathrm{E}(\varphi_\mathrm{v})/\mathrm{RT}} \quad (5)$$

In other words, while according to equation (4), K, n and E are not dependent on the ϕ_v, equation (5) explicitly models and allows to compute the dependence of n and E on the solid loading. The scientific literature on the rheology of mixtures makes sometimes use of a mouldability index. Abolhasani and Muhamad (2009) proposed a mouldability index which is a compact combination of the K, n and E parameters of the rheological model. The value of n indicates the degree of shear rate sensitivity of the feedstock. Larger n-values (i.e. reduced shear rate sensitivity) are generally preferred for solid-binder mixtures, because they reduce segregation problems (Khakbiz et al., 2005). Similarly, smaller E-values are preferred because they reduce the rheological influence of temperature and make the extrusion process more stable and controllable. However, in vertical extrusion of filaments the role of K is less relevant, and the effects of n and E can be better analysed separately. The resulting E- and n-values are plotted in Figure 6. The increasing trend of n-value with increasing solid loading indicates that larger ϕ_v values yield better shear rate sensitivity (larger n-value) but worse temperature sensitivity. From a technological point of view, the n value is more important than E, because shear rate variations could be appreciated during a single extrusion stroke in real operations, while temperature changes are slower and should not influence the within-part process variation. Therefore, capillary rheometry suggests that higher solid loading should be preferred, within the investigated range, to enhance stability. Besides, as clearly shown in Figure 5, mixtures with higher solid loading are more viscous, hence they should be more stable in extrusion.

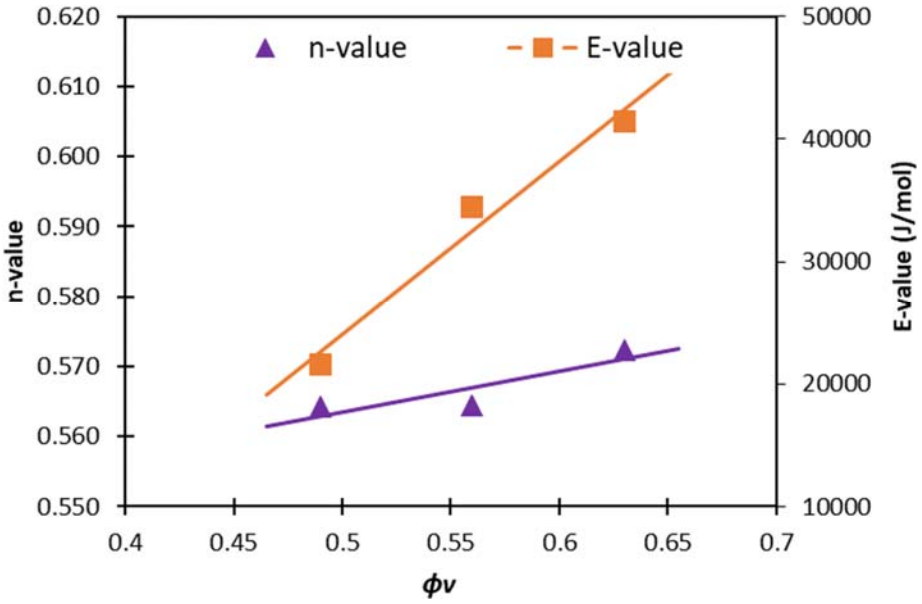

Figure 6: n- and E-values as a function of solid loading for the as-extruded feedstock

3.3 Extrudability as a function of shear rate

The same approach used in Section 3.2 for investigating the extrudability with respect to solid loading, can now be used for the shear rate. Another 3-parameters model can be built as a modification of equation (4), grouping the data by shear rate value, so that the dependence of the m and E on $\dot{\gamma}$ explicitly emerges:

$$\eta = \mathrm{K}(\dot{\gamma})\left(1 - \frac{\varphi_v}{\varphi_{v\_max}}\right)^{-\mathrm{m}(\dot{\gamma})} \mathrm{e}^{\mathrm{E}(\dot{\gamma})/\mathrm{RT}} \qquad (6)$$

A very interesting relationship between m and E and the shear rate is found. The resulting values are plotted in Figure 7, which shows a strongly non-linear trend. In the low shear rate regime, the flow activation energy E increases with $\dot{\gamma}$, and this is in agreement with some other findings in the scientific literature (Huang et al., 2003). In the high shear rate regime, E decreases with $\dot{\gamma}$, and this is also in agreement with the literature (Khakbiz et al., 2005).

It can be observed that there is a non-trivial conflict between E and m: when the sensitivity to the powder loading increases, the E-value decreases (improves). As stated before about the relative technological importance of n and E, here again the m-value can be considered more important than E, because minor homogeneity and composition variations could be appreciated within a single extruded filament in real operations, while temperature changes are slow. The best (smallest) m-values are obtained for relatively low shear rates, between 100 and 600 s^{-1}. Besides, as

clearly shown in Figure 5, mixtures tested at lower shear rates are more viscous, hence they should be more stable in extrusion.

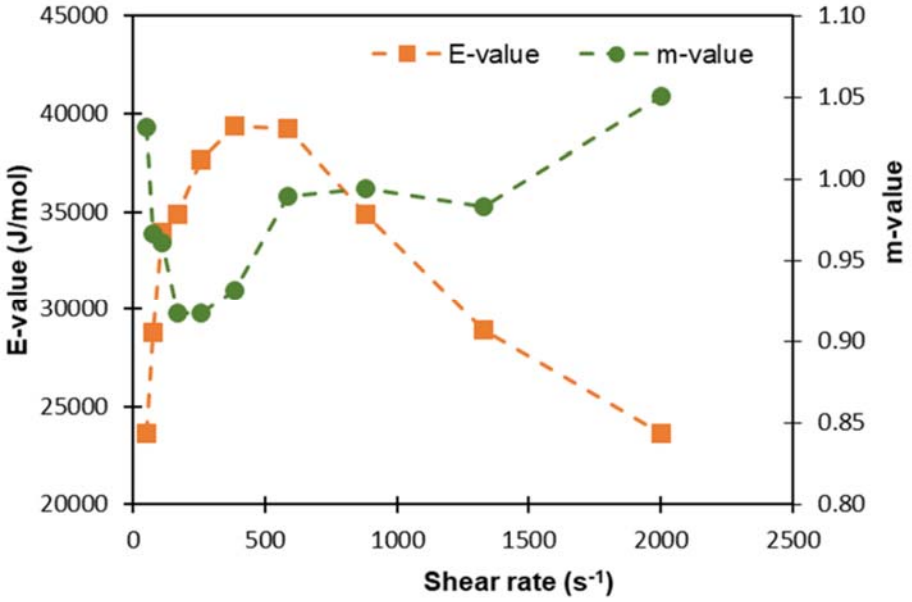

Figure 7: m- and E-values vs. the shear rate for the as-extruded feedstock

In conclusion, the rheological results indicate that optimal conditions can be found, for the investigated feedstock, where the theoretical extrudability is maximized. The best conditions should be obtained for ϕ_v selected at the maximum value of the range (0.63) and for shear rate $\dot{\gamma}$ below 500 s^{-1}. This prediction simply derives by looking at the values taken by the rheological constants results and the viscosity. The actual stability of the vertical extrusion process must be assessed by means of dedicated extrusion tests, by considering the stability of the pressure vs. time signals during extrusion and the dimensional variability of the extruded filaments. The results of the extrusion tests are described in the following Section.

4. Results and discussion of extrusion tests

In the previous Section 3 we have discussed the extrudability of the metal-binder mixtures starting from their rheological properties. The aim of the present Section is to verify the behavior of the materials in an actual extrusion process. For this reason, extrusion tests have been run with the equipment shown in Figure 3 (b), using the nozzles shown in Figure 4. A total of 120 tests has been run (4 temperature levels, 2 nozzle diameters, 3 powder loading, 5 piston speeds), following the plan of conditions listed in Table 2. The results are presented and discussed in Section

4.1. The extrusion unit shown in Figure 3 can be combined with a robotic deposition table, as described in (Rane et al., 2019). This enables the realization of an Extrusion based Additive Manufacturing (EAM) process, which requires a stable and controllable flow of extruded material. The stability conditions have important implications on the whole EAM process chain, which are discussed in Section 4.1

4.1. Stability of the extrusion process

The first purpose of the tests is to verify what extrusion conditions yield the best results in terms of stability of the pressure curves. Since the CNC extrusion unit is stroke-controlled, i.e. the output shear rate and flow rate should be constant throughout the process, the electric load required at the electric drive can fluctuate, i.e. the pressure at the nozzle can have fluctuations. For each test, the shear rate $\dot{\gamma}$ can be estimated according to equation (1). In Figure 8, some example of pressure vs. time curves are shown.

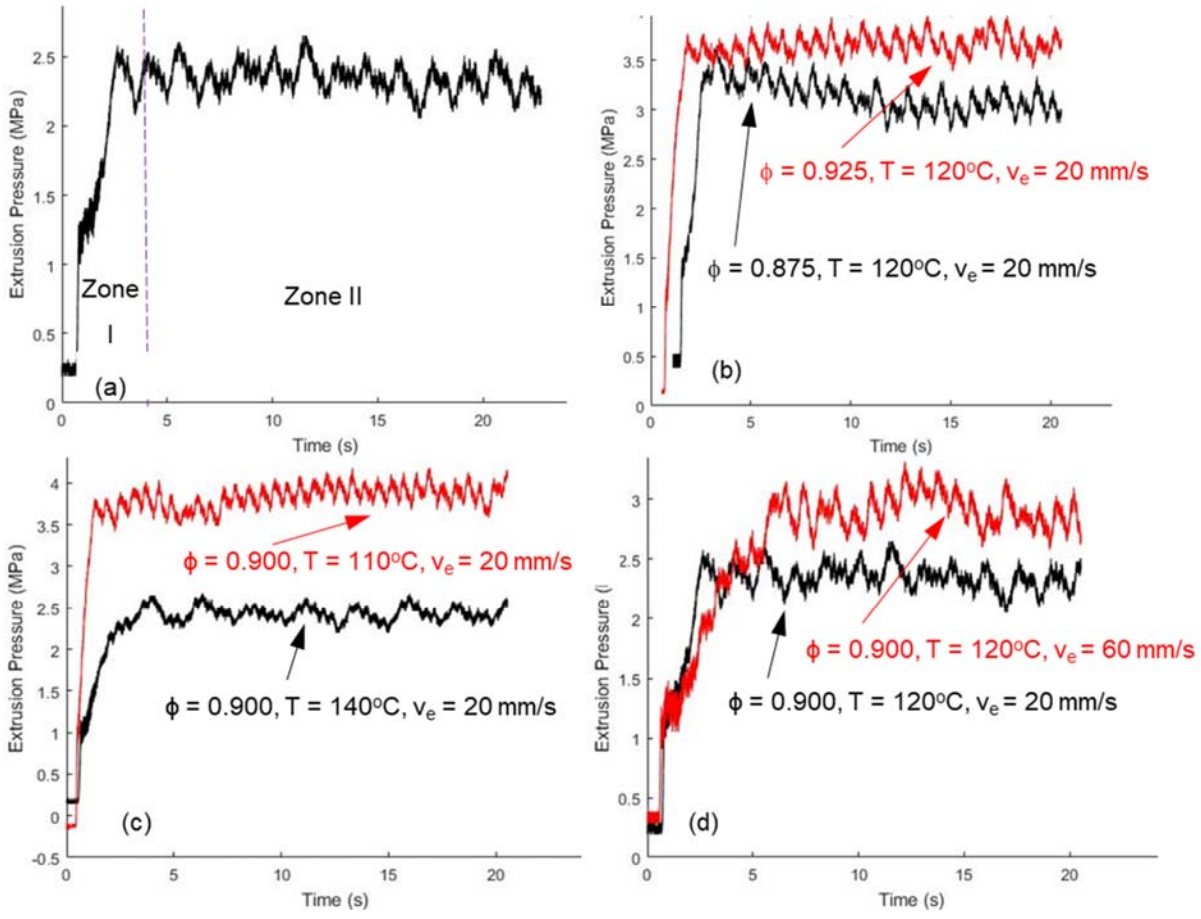

Figure 8: Examples of pressure vs. time curves during the extrusion tests

All curves have an initial ramp-up region (Zone I in Figure 8 (a)), then they stabilize to an average constant value (Zone II). The signal has first been trimmed, discarding the first 1/5 of the acquisition, to isolate the data of zone II. Then, the signal has been smoothened by a low-pass filter, cutting all frequencies above 25 Hz, to remove any electrical noise and focus onto the actual variation of pressure. Then, the average pressure P value of each signal has been calculated in zone II. The oscillation ΔP (MPa) between the minimum and the maximum values in zone II has also been calculated. The ratio ΔP/P can be used as an indicator of the stability of the extrusion process. During some tests, pressure oscillation ΔP/P as large as 0.45 have been observed. The ΔP/P has not been quantitatively correlated to the dimensional variations, the quality of the actual flow rate of the extruded filaments. However, a maximum acceptable ΔP/P level of 0.3 could be assessed as the limit above which the process becomes too unstable.

In order to model the dependence of $\Delta P/P$ on the extrusion parameters, a full quadratic regression model has been developed. The most relevant and interesting result of the model is a strong interacting effect between the estimated shear rate $\dot{\gamma}$ and the powder loading ϕ_v, but also between the temperature T and the powder loading ϕ_v. These two interactions can be appreciated in the contour plots given in Figure 9. In Figure 9 (a), a contour plot of $\Delta P/P$ is given, as a function of solid loading and ϕ_v and shear rate $\dot{\gamma}$. Darker regions indicate larger pressure fluctuations and process instability. The thick red line shows the boundary between the acceptable region and the unstable region. The figure shows that a larger solid loading makes the pressure signal more stable; when ϕ_v exceeds 0.56 the process is below the 0.3 limit at nearly all shear rates.

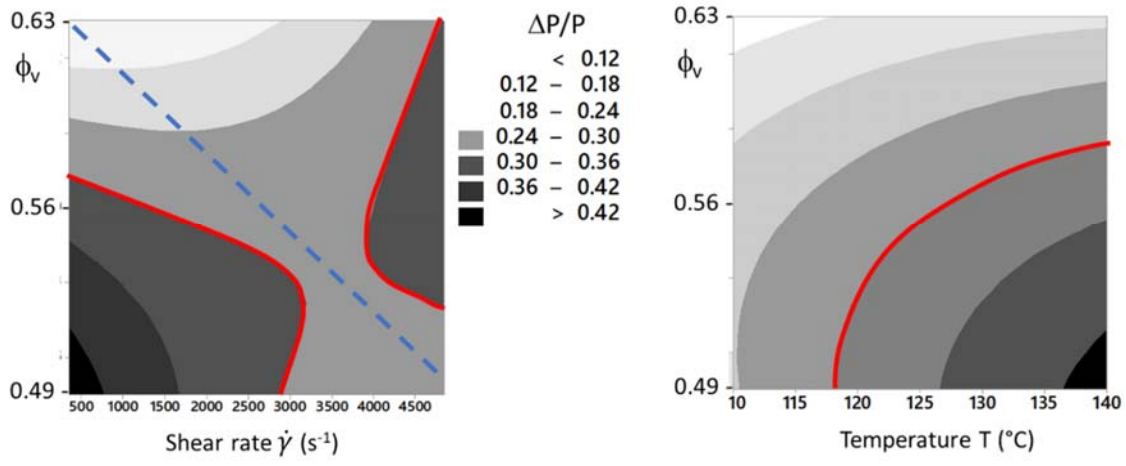

Figure 9: Contour plots of ΔP/P vs. ϕ_v and $\dot{\gamma}$ (left, hold temperature T=125 °C) and of $\Delta P/P$ vs. T and $\dot{\gamma}$ (right, hold shear rate $\dot{\gamma} = 1828\ s^{-1}$) after the regression model of extrusion tests

With a further observation of the plot, for each ϕ_v level there is an optimal shear rate which decreases as ϕ increases. The optimal shear rate locus is represented as a dotted line in Figure 9 (a).

In Figure 9 (b), a contour plot of $\Delta P/P$ is given, as a function of solid loading and ϕ_v and temperature T. The figure shows that as temperature increases, the pressure signal becomes more unstable; however, feedstock with the larger solid loading is less influenced by a temperature variation in the investigated range. When ϕ_v exceeds 0.56 the process is stable at any temperature.

In order to further verify the effect of T, ϕ_v and $\dot{\gamma}$ on the stability of the process, additional extrusion tests have been run, using the within-filament coefficient of variation of the extruded diameter σ_D/D as the response variable. Again, a statistical regression analysis has been conducted, applying a logarithmic transformation of the response variable σ_D/D in order to normalize the residual errors. Although the linear regression model obtained has a large standard error, i.e. the data are affected by large scatter, there is a clear statistical significance of the three investigated factors. The most influent factor is the powder loading, the second most influent parameter is the extrusion temperature T and, finally, there is a minor influence of the shear rate (process more stable at smaller shear rates). For a more effective graphical representation of the data, in Fig. 10 the independent parameter $\dot{\gamma}$ has been replaced with the shear viscosity, estimated by equation (4). While each group of data in Fig. 10 is affected by a large scatter, the figure still indicates some clear (and statistically tested) trends. As observed for the pressure signal, the more viscous feedstock $\phi_v = 0.63$ yields more stable results, also in terms of diameter variation. As for the temperature T, the extruded filaments are dimensionally more uniform (i.e. more stable) when T is lower. The combined effects of T, ϕ_v and $\dot{\gamma}$ all point towards a weak negative correlation of σ_D/D with the apparent viscosity. In other words, a feedstock which is more viscous either because it has a larger solid loading or because it is extruded at a smaller temperature or because it is extruded at a slower shear rate, will produce a more uniform filament.

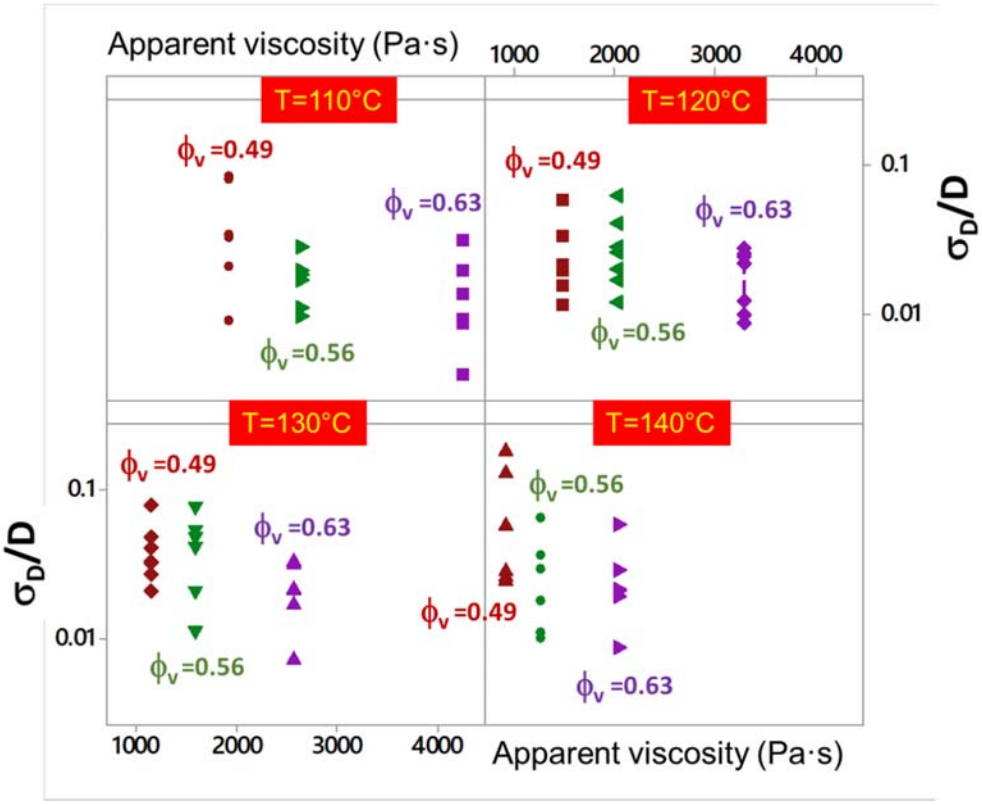

Figure 10: Correlation among the estimated viscosity and the coefficient of variation σ_D/D of the extruded filament diameter (plotted in log scale)

4.2. Implications on the 3d printing process

The extrusion tests have demonstrated that the vertical extrusion process is more stable when the filaments have larger solid loading, when they are extruded at small temperature, when they are extruded at lower shear rates. These conditions have implications on the deposition of the extruded filaments during the Extrusion based Additive Manufacturing (EAM) process. The need for highly viscous mixtures has important implications on equipment, on productivity and on quality of 3d printed parts. In order to easily extrude highly viscous mixtures, powerful and stable extruders are required. This reduces the range of applications for simple and low cost 3d printing machines. With respect to quality, the adhesion between layers and roads is negatively affected by a high solid loading, because of a lower amount of polymeric fraction. Similarly, extruding at a smaller temperature reduces the adhesion between layers. This suggests that the 3d printing table should be enclosed in a temperature-controlled chamber, in order to prevent rapid cooling and to improve adhesion. Finally, extruding at lower shear rates makes the 3d printing process easier to be controlled, because of slower kinematics. However, this reduces the build-up time and the productivity.

Finally, it can be observed that feedstock with higher solid loading can be more easily debinded and sintered, yielding larger final densities.

5. Conclusions

Rheological tests (using Capillary Rheometer) and vertical extrusion tests have been conducted with mixtures of stainless steel powder and polymeric binder. The mixtures have been tested as-mixed and after a first extrusion. The results demonstrate that the feedstock after the first extrusion is more stable and more homogeneous, thanks to an increased consistency, but especially thanks to a reduced sensitivity to powder loading.

If considering the as-extruded feedstocks only, according to their rheological parameters and the measured viscosity values, the predicted region of optimal extrudability should be with a feedstock with a solid loading of 63% by volume, extruded in the lower temperature range and with a low shear rate, below 500 s^{-1}.

According to the vertical extrusion tests, the pressure signal is more stable for the 63% formulation; this agrees with the prediction of the rheological tests. The extrusion tests also confirm that the pressure signal is more stable at lower temperature. Furthermore, the extrusion tests indicate that there is an optimal shear rate which decreases as ϕ_v increases and that the feedstock with the larger solid loading is less sensitive to temperature variations.

Finally, in terms of dimensional stability of the extruded filaments, the tests indicate that the process is more stable when the viscosity is increased, i.e. when temperature and shear rate are lower and when the solid loading is higher.

6. References

Abolhasani, H., Muhamad, N., 2009. Rheological investigation of a starch-based binder and feedstock for metal injection molding. Int. J. Mech. Mater. Eng. 4, 294–299.

Agote, I., Odriozola, A., Gutierrez, M., Santamaría, A., Quintanilla, J., Coupelle, P., Soares, J., 2001. Rheological study of waste porcelain feedstocks for injection moulding. J. Eur. Ceram. Soc. 21, 2843–2853. https://doi.org/10.1016/S0955-2219(01)00210-2

Annoni, M., Giberti, H., Strano, M., 2016. Feasibility Study of an Extrusion-based Direct Metal Additive Manufacturing Technique. Procedia Manuf. 5, 916–927. https://doi.org/10.1016/j.promfg.2016.08.079

Berginc, B., Brezo, M., Kampu, Z., 2009. A Numerical Simulation of Metal Injection Moulding. Mater. Tehnol. / Mater. Technol. 43, 43–48.

Bose, A., Schuh, C.A., Tobia, J.C., Tuncer, N., Mykulowycz, N.M., Preston, A., Barbati, A.C., Kernan, B., Gibson, M.A., Krause, D., Brzezinski, T., Schroers, J., Fulop, R., Myerberg, J.S., Sowerbutts, M., Chiang, Y.M., John Hart, A., Sachs, E.M., Lomeli, E.E., Lund, A.C., 2018. Traditional and additive manufacturing of a new Tungsten heavy alloy alternative. Int. J. Refract. Met. Hard Mater. 73, 22–28. https://doi.org/10.1016/j.ijrmhm.2018.01.019

Cheng, J., Wan, L., Cai, Y., Zhu, J., Song, P., Dong, J., 2010. Fabrication of W-20 wt.%Cu alloys by powder injection molding. J. Mater. Process. Technol. 210, 137–142. https://doi.org/10.1016/j.jmatprotec.2009.08.001

Contreras, J.M., Jiménez-Morales, A., Torralba, J.M., 2010. Experimental and theoretical methods for optimal solids loading calculation in MIM feedstocks fabricated from powders with different particle characteristics. Powder Metall. 53, 34–40. https://doi.org/10.1179/003258909X12450768327225

Faes, M., Valkenaers, H., Vogeler, F., Vleugels, J., Ferraris, E., 2015. Extrusion-based 3D printing of ceramic components. Procedia CIRP 28, 76–81. https://doi.org/10.1016/j.procir.2015.04.028

Gelin, J.C., Barriere, T., Dutilly, M., 1999. Experiments and Computational Modeling of Metal Injection Molding for Forming Small Parts. CIRP Ann. - Manuf. Technol. 48, 179–182. https://doi.org/10.1016/S0007-8506(07)63160-6

Giberti, H., Strano, M., Annoni, M., 2016. An innovative machine for Fused Deposition Modeling of metals and advanced ceramics, in: MATEC Web of Conferences. Les Ulis. https://doi.org/10.1051/mateccont/20164303003

Gonzalez-Gutierrez, J., Duretek, I., Kukla, C., Poljšak, A., Bek, M., Emri, I., Holzer, C., 2016. Models to Predict the Viscosity of Metal Injection Molding Feedstock Materials as Function of Their Formulation. Metals (Basel). 6, 129. https://doi.org/10.3390/met6060129

Hidalgo, J., Jiménez-Morales, A., Barriere, T., Gelin, J.C., Torralba, J.M., 2014. Water soluble Invar 36 feedstock development for μpIM. J. Mater. Process. Technol. 214, 436–444. https://doi.org/10.1016/j.jmatprotec.2013.09.014

Huang, B., Liang, S., Qu, X., 2003. The rheology of metal injection molding. J. Mater. Process. Technol. 137, 132–137. https://doi.org/10.1016/S0924-0136(02)01100-7

Ismael, M.R., Clemens, F., Graule, T., Hoffmann, M.J., 2011. Effects of different thermoplastic binders on the processability of feedstocks for ceramic co-extrusion process. Ceram. Int. 37, 3173–3182. https://doi.org/10.1016/j.ceramint.2011.05.084

Khakbiz, M., Simchi, A., Bagheri, R., 2005. Analysis of the rheological behavior and stability of 316L stainless steel–TiC powder injection molding feedstock. Mater. Sci. Eng. A 407, 105–113. https://doi.org/10.1016/j.msea.2005.06.057

Kong, X., Barriere, T., Gelin, J.C.C., 2012. Determination of critical and optimal powder loadings for 316L fine stainless steel feedstocks for micro-powder injection molding. J. Mater. Process. Technol. 212, 2173–2182. https://doi.org/10.1016/j.jmatprotec.2012.05.023

Kuang, Y., Ngai, T.L., Luo, H., Li, Y., 2009. SiC-Ti layered material prepared by binder-treated powder sintering. J. Mater. Process. Technol. 209, 4607–4610. https://doi.org/10.1016/j.jmatprotec.2008.11.033

Machaka, R., Ndlangamandla, P., Seerane, M., 2018. Capillary rheological studies of 17-4 PH MIM feedstocks prepared using a custom CSIR binder system. Powder Technol. 326, 37–43. https://doi.org/10.1016/j.powtec.2017.12.051

Ochoa, I., Hatzikiriakos, S.G., 2005. Paste extrusion of polytetrafluoroethylene (PTFE): Surface tension and viscosity effects. Powder Technol. 153, 108–118. https://doi.org/10.1016/j.powtec.2005.02.007

Özgün, Ö., Gülsoy, H.Ö., Findik, F., Yilmaz, R., 2012. Microstructure and mechanical properties of injection moulded Nimonic-90 superalloy parts. Powder Metall. 55, 405–414. https://doi.org/10.1179/1743290112Y.0000000010

Parenti, P., Kuriakose, S., Mussi, V., Strano, M., Annoni, M., 2017. Green-state micromilling of AISI316L feedstock, in: 2017 World Congress on Micro and Nano Manufacturing (WCMNM 2017)

Pettas, D., Karapetsas, G., Dimakopoulos, Y., Tsamopoulos, J., 2015. On the origin of extrusion instabilities: Linear stability analysis of the viscoelastic die swell. J. Nonnewton. Fluid Mech. 224, 61–77. https://doi.org/10.1016/j.jnnfm.2015.07.011

Rane, K., Castelli, K., Strano, M., 2019. Rapid surface quality assessment of green 3D printed metal-binder parts. J. Manuf. Process. 38, 290–297. https://doi.org/10.1016/j.jmapro.2019.01.032

Raza, M.R., Ahmad, F., Omar, M.A., German, R.M., 2012. Effects of cooling rate on mechanical properties and corrosion resistance of vacuum sintered powder injection molded 316L stainless steel. J. Mater. Process. Technol. 212, 164–170. https://doi.org/10.1016/j.jmatprotec.2011.08.019

Royer, A., Barriere, T., Gelin, J.C., 2015. The degradation of poly(ethylene glycol) in an Inconel 718 feedstock in the metal injection moulding process. Powder Technol. 284, 467–474. https://doi.org/10.1016/j.powtec.2015.07.032

Samanta, S.K., Chattopadhyay, H., Godkhindi, M.M., 2011. Thermo-physical characterization of binder and feedstock for single and multiphase flow of PIM 316L feedstock. J. Mater. Process. Technol. 211, 2114–2122. https://doi.org/10.1016/j.jmatprotec.2011.07.008

Sidambe, A.T., Figueroa, I.A., Hamilton, H.G.C., Todd, I., 2012. Metal injection moulding of CP-Ti components for biomedical applications. J. Mater. Process. Technol. 212, 1591–1597. https://doi.org/10.1016/j.jmatprotec.2012.03.001

Sotomayor, M., E., Levenfeld, B., 2010. Powder extrusion moulding of 430L stainless steel thin tubes for porous metal supported SOFCs. Powder Metall. https://doi.org/10.1179/003258909X12502679013693

Suri, P., Atre, S. V., German, R.M., de Souza, J.P., 2003. Effect of mixing on the rheology and particle characteristics of tungsten-based powder injection molding feedstock. Mater. Sci. Eng. A 356, 337–344. https://doi.org/10.1016/S0921-5093(03)00146-1

Thavanayagam, G., Pickering, K.L., Swan, J.E., Cao, P., 2015. Analysis of rheological behaviour of titanium feedstocks formulated with a water-soluble binder system for powder injection moulding. Powder Technol. 269, 227–232. https://doi.org/10.1016/j.powtec.2014.09.020

Zaky, M.T., Soliman, F.S., Farag, A.S., 2009. Influence of paraffin wax characteristics on the formulation of wax-based binders and their debinding from green molded parts using two comparative techniques. J. Mater. Process. Technol. 209, 5981–5989. https://doi.org/10.1016/j.jmatprotec.2009.07.018

Zauner, R., Binet, C., Heaney, D.F., Piemme, J., 2004. Variability of feedstock viscosity and its correlation with dimensional variability of green powder injection moulded components. Powder Metall. 47, 150–155. https://doi.org/10.1179/003258904225015473